A multicenter phase II study of carboplatin and paclitaxel for advanced thymic carcinoma: WJOG4207 L.	Hirai F, Yamanaka T, Taguchi K, Daga H, Ono A, Tanaka K, Kogure Y, Shimizu J, Kimura T, Fukuoka J, Iwamoto Y, Sasaki H, Takeda K, Seto T, Ichinose Y, Nakagawa K, Nakanishi Y; for the West Japan Oncology Group.	Ann Oncol. 2014 Nov 17. pii: mdu541.	2014 Nov	国外
Multicentre analysis of long-term outcome after surgical resection for gastric cancer liver metastases.	Kinoshita T, Kinoshita T, Saiura A, Esaki M, Sakamoto H, Yamanaka T.	Br J Surg. 2015 Jan;102(1):102-7.	2015 Jan	国外
Erlotinib alone or with bevacizumab as first-line therapy in patients with advanced non-squamous non-small-cell lung cancer harbouring EGFR mutations (JO25567): an open-label, randomised, multicentre, phase 2 study.	Seto T, Kato T, Nishio M, Goto K, Atagi S, Hosomi Y, Yamamoto N, Hida T, Maemondo M, Nakagawa K, Nagase S, Okamoto I, Yamanaka T, Tajima K, Harada R, Fukuoka M, Yamamoto N.	Lancet Oncol 2014 Oct;15(11):1236-44.	2014 Oct	国外

A phase II study of five peptides combination with oxaliplatin-based chemotherapy as a first-line therapy for advanced colorectal cancer (FXV study).	Hazama S, Nakamura Y, Tanaka H, Hirakawa K, Tahara K, Shimizu R, Ozasa H, Etoh R, Sugiura F, Okuno K, Furuya T, Nishimura T, Sakata K, Yoshimatsu K, Takenouchi H, Tsunedomi R, Inoue Y, Kanekiyo S, Shindo Y, Suzuki N, Yoshino S, Shinozaki H, Kamiya A, Furukawa H, Yamanaka T, Fujita T, Kawakami Y, Oka M.	J Transl Med. 2014 Apr 30;12:108. doi: 10.1186/1479-5876-12-108.		国外
Risk factors for pericardial effusion in patients with stage I esophageal cancer treated with chemoradiotherapy.	Tamari K, Isohashi F, Akino Y, Suzuki O, Seo Y, Yoshioka Y, Hayashi Y, Nishida T, Takehara T, Mori M, Doki Y, Ogawa K.：	Anticancer Res. 2014 Dec;34(12):7389-93.	2014 Dec	国外

Efficacy and safety of nedaplatin-based concurrent chemoradiotherapy for FIGO Stage IB2-IVA cervical cancer and its clinical prognostic factors.	Fujiwara M, Isohashi F, Mabuchi S, Yoshioka Y, Seo Y, Suzuki O, Sumida I, Hayashi K, Kimura T, Ogawa K.	J Radiat Res 2014 Nov 26. pii: rru101.	2014 Nov	国外
Treatment outcomes using CyberKnife for brain metastases from lung cancer.	Tamari K, Suzuki O, Hashimoto N, Kagawa N, Fujiwara M, Sumida I, Seo Y, Isohashi F, Yoshioka Y, Yoshimine T, Ogawa K.	J Radiat Res. 2014 Oct 25. pii: rru092.	2014 Oct	国外
Hypofractionated stereotactic radiotherapy using CyberKnife as a boost treatment for head and neck cancer, a multi-institutional survey: impact of planning target volume.	Yamazaki H, Ogita M, Himei K, Nakamura S, Yoshida K, Kotsuma T, Yamada Y, Fujiwara M, Baek S, Yoshioka Y.	Anticancer Res 2014 Oct;34(10):5755-9.	2014 Oct	国外

A preliminary results of MRI-assisted high-dose-rate interstitial brachytherapy for uterine cervical cancer.	Yoshida K, Yamazaki H, Takenaka T, Kotsuma T, Miyake S, Mikami Ueda M, Yoshida M, Masui K, Yoshioka Y, Uesugi Y, Shimbo T, Yoshikawa N, Yoshioka H, Aramoto K, Narumi Y, Yamada S, Tatsumi K, Tanaka E.	Brachytherapy. 2014 Sep 10. pii: S1538-4721(14)00588-1. doi: 10.1016/j.brachy.2014.07.006.	2014 Sept	国外
Transitioning from conventional radiotherapy to intensity-modulated radiotherapy for localized prostate cancer: changing focus from rectal bleeding to detailed quality of life analysis.	Yamazaki H, Nakamura S, Nishimura T, Yoshida K, Yoshioka Y, Koizumi M, Ogawa K.	J Radiat Res 2014 Nov;55(6):1033-47.	2014 Nov	国外
Comparison of acute and subacute genitourinary and gastrointestinal adverse events of radiotherapy for prostate cancer using intensity-modulated radiation therapy, three-dimensional conformal radiation therapy, permanent implant	Morimoto M, Yoshioka Y, Konishi K, Isohashi F, Takahashi Y, Ogata T, Koizumi M, Teshima T, Bijl HP, van der Schaaf A, Langendijk JA, Ogawa K.	Tumori. 2014 May-Jun;100(3):265-71.	2014 May-Jun	国外

brachytherapy and high-dose-rate brachytherapy.				
Longitudinal analysis of late vaginal mucosal reactions after high-dose-rate brachytherapy in patients with gynecological cancer.	Yoshida K, Yamazaki H, Nakamura S, Masui K, Kotsuma T, Akiyama H, Tanaka E, Narumi Y, Yoshioka Y.	Anticancer Res. 2014 Aug;34(8):4433-8.	2014 Aug	国外
Impact of intraluminal brachytherapy on survival outcome for radiation therapy for unresectable biliary tract cancer: a propensity-score matched-pair analysis.	Yoshioka Y, Ogawa K, Oikawa H, Onishi H, Kanesaka N, Tamamoto T, Kosugi T, Hatano K, Kobayashi M, Ito Y, Takayama M, Takemoto M, Karasawa K, Nagakura H, Imai M, Kosaka Y, Yamazaki H, Isohashi F, Nemoto K, Nishimura Y; Japanese Radiation Oncology Study Group (JROSG).	Int J Radiat Oncol Biol Phys 2014 Jul 15;89(4):822-9.	2014 Jul	国外

Dosimetry analyses comparing high-dose-rate brachytherapy, administered as monotherapy for localized prostate cancer, with stereotactic body radiation therapy simulated using CyberKnife.	Fukuda S, Seo Y, Shiomi H, Yamada Y, Ogata T, Morimoto M, Konishi K, Yoshioka Y, Ogawa K.	J Radiat Res 2014 Nov;55(6):1114-21.	2014 Nov	国外
Role of novel risk classification method, Prostate Cancer Risk Index (PRIX) for clinically localized prostate cancer after high-dose-rate interstitial brachytherapy as monotherapy.	Yoshida K, Yamazaki H, Nakamura S, Masui K, Kotsuma T, Akiyama H, Tanaka E, Yoshioka Y.	Anticancer Res 2014 Jun;34(6):3077-81.	2014 Jun	国外
High-dose-rate interstitial brachytherapy for mobile tongue cancer: preliminary results of a dose reduction trial.	Akiyama H, Yoshida K, Yamazaki H, Takenaka T, Kotsuma T, Masui K, Yoshioka Y, Arika T, Shimizutani K, Tanaka E.	J Contemp Brachytherapy. 2014 Mar;6(1):10-4.	2014 Mar	国外
Comparison of common terminology criteria for adverse events v3.0 and radiation therapy oncology group toxicity score system after high-dose-rate interstitial	Yoshida K, Yamazaki H, Nakamara S, Masui K, Kotsuma T, Akiyama H, Tanaka E, Yoshioka Y	Anticancer Res 2014 Apr;34(4):2015-8.	2014 Apr	国外

brachytherapy as monotherapy for prostate cancer.				
Factors influencing survival outcome for radiotherapy for biliary tract cancer: a multicenter retrospective study.	Yoshioka Y, Ogawa K, Oikawa H, Onishi H, Uchida N, Maebayashi T, Kanesaka N, Tamamoto T, Asakura H, Kosugi T, Hatano K, Yoshimura M, Yamada K, Tokumaru S, Sekiguchi K, Kobayashi M, Soejima T, Isohashi F, Nemoto K, Nishimura Y; Japanese Radiation Oncology Study Group.	Radiother Oncol. 2014 Mar;110(3):546-52.	2014 Mar	国外

Impact of stereotactic body radiotherapy on colorectal cancer with distant metastases.	Hiraki M, Nishimura J, Ohtsuka M, Shiomi H, Uemura M, Haraguchi N, Hata T, Hayashi T, Takemasa I, Mizushima T, Isohashi F, Yoshioka Y, Ogawa K, Doki Y, Mori M, Yamamoto H.	Oncol Rep. 2014 Feb;31(2):795-9.	2014 Feb	国外
Monotherapeutic high-dose-rate brachytherapy for prostate cancer: a dose reduction trial.	Yoshioka Y, Konishi K, Suzuki O, Nakai Y, Isohashi F, Seo Y, Otani Y, Koizumi M, Yoshida K, Yamazaki H, Nonomura N, Ogawa K.	Radiother Oncol 2014 Jan;110(1):114-9.	2014 Jan	国外
Evaluation of imaging performance of megavoltage cone-beam CT over an extended period.	Sumida I, Yamaguchi H, Kizaki H, Yamada Y, Koizumi M, Yoshioka Y, Ogawa K, Kakimoto N, Murakami S, Furukawa S.	J Radiat Res 2014 Jan 1;55(1):191-9.	2014 Jan	国外

Patterns of practice in the radiation therapy for bladder cancer: survey of the Japanese Radiation Oncology Study Group (JROSG)..	Maebayashi T, Ishikawa H, Yorozu A, Yoshida D, Katoh H, Nemoto K, Ishihara S, Takemoto S, Ishibashi N, Tokumaru S, Akimoto T; Working Subgroup of Urological Cancers in Japanese Radiation Oncology Study Group.	Jpn J Clin Oncol 2014 Nov;44(11):1109-15	2014 Nov	国外
Permanent prostate brachytherapy with or without supplemental external beam radiotherapy as practiced in Japan: Outcomes of 1300 patients.	Yorozu A, Kuroiwa N, Takahashi A, Toya K, Saito S, Nishiyama T, Yagi Y, Tanaka T, Shiraishi Y, Ohashi T.	Brachytherapy. 2014 Aug 7. pii: S1538-4721(14)00573-X. doi: 10.1016/j.brachy.2014.06.008.	2014 Aug	国外
Nationwide Japanese Prostate Cancer Outcome Study of Permanent Iodine-125 Seed Implantation (J-POPS).	Saito S, Ito K, Yorozu A, Aoki M, Koga H, Satoh T, Ohashi T, Shigematsu N, Maruo S, Kikuchi T, Kojima S, Dokiya T, Fukushima M, Yamanaka H.	Int J Clin Oncol. 2014 May 21.	2014 May	国外

Assessing protection against radiation exposure after prostate (125)I brachytherapy.	Hanada T, Yorozu A, Kikumura R, Ohashi T, Shigematsu N.	Brachytherapy. 2014 May-Jun;13(3):311-8. doi: 10.1016/j.brachy.2013.12.001.	2014 May-Jun	国外
Combined brachytherapy and external beam radiotherapy without adjuvant androgen deprivation therapy for high-risk prostate cancer.	Ohashi T, Yorozu A, Saito S, Momma T, Nishiyama T, Yamashita S, Shiraishi Y, Shigematsu N.	Radiat Oncol. 2014 Jan 9;9:13. doi: 10.1186/1748-717X-9-13.	2014 Jan	国外

International Journal of
Radiation Oncology
biology • physics

www.redjournal.org

Clinical Investigation: Lymphoma

Localized Ocular Adnexal Mucosa-Associated Lymphoid Tissue Lymphoma Treated With Radiation Therapy: A Long-Term Outcome in 86 Patients With 104 Treated Eyes

Ken Harada, MD,* Naoya Murakami, MD, PhD,* Mayuka Kitaguchi, MD,* Shuhei Sekii, MD,* Kana Takahashi, MD,* Kotaro Yoshio, MD, PhD,* Koji Inaba, MD,* Madoka Morota, MD, PhD,* Yoshinori Ito, MD,* Minako Sumi, MD, PhD,* Shigenobu Suzuki, MD,† Kensei Tobinai, MD, PhD,‡ Takashi Uno, MD, PhD,§ and Jun Itami, MD, PhD*

*Departments of *Radiation Oncology, †Ophthalmic Oncology, and ‡Hematologic Oncology, National Cancer Center Hospital, Tokyo; and §Department of Radiology, Chiba University School of Medicine, Chiba, Japan*

Received Sep 25, 2013, and in revised form Nov 10, 2013. Accepted for publication Nov 12, 2013.

Summary

Eighty-six patients with histologically proven stage I primary ocular adnexal mucosa-associated lymphoid tissue (MALT) lymphoma (POAML) treated with radiation therapy at National Cancer Center Hospital, Tokyo between 1990 and 2010 were retrospectively reviewed. The majority of patients with POAML showed behavior consistent with that of localized, indolent diseases. Thirty gray of local irradiation seems to be quite effective. The initial bilateral involvement and contralateral orbital relapses can be also controlled with

Purpose: To evaluate the natural history, behavior of progression, prognostic factors, and treatment-related adverse effects of primary ocular adnexal mucosa-associated lymphoid tissue (MALT) lymphoma (POAML).

Methods and Materials: Eighty-six patients with histologically proven stage I POAML treated with radiation therapy at National Cancer Center Hospital, Tokyo between 1990 and 2010 were retrospectively reviewed. The median age was 56 years (range, 18-85 years). The median dose administered was 30 Gy (range, 30-46 Gy). Seventy-seven patients (90%) were treated by radiation therapy alone.

Results: The median follow-up duration was 9 years (range, 0.9-22 years). The 5- and 10-year overall survival (OS) rates were 97.6% and 93.5%, respectively, and no patients died of lymphoma. Patients with tumor sizes $\geq$4 cm showed a greater risk of contralateral relapse (P=.012). Six patients with contralateral relapse were seen and treated by radiation therapy alone, and all the lesions were controlled well, with follow-up times of 3 to 12 years. There was 1 case of local relapse after radiation therapy alone, and 3 cases of relapse occurred in a distant site. Cataracts developed in 36 of the 65 eyes treated without lens shielding and in 12 of the 39 patients with lens shielding (P=.037).

Conclusions: The majority of patients with POAML showed behavior consistent with that of localized, indolent diseases. Thirty gray of local irradiation seems to be quite effective. The initial bilateral involvement and contralateral orbital relapses can be also controlled with radiation therapy alone. Lens shielding reduces the risk of cataract.

Reprint requests to: Ken Harada, MD, Department of Radiation Oncology, National Cancer Center Hospital, 5-1-1, Chuo-ku, Tsukiji, Tokyo, Japan 104-0045. Tel: (+81) 3-3542-2511; E-mail: keharada@ncc.go.jp

Conflict of interest: none.

Int J Radiation Oncol Biol Phys, Vol. 88, No. 3, pp. 650–654, 2014
0360-3016/$ - see front matter
http://dx.doi.org/10.1016/j.ijrobp.2013.11.235

radiation therapy alone. Lens shielding reduces the risk of cataract.

Introduction

The incidence of ocular adnexal lymphoma is reported to be less than 10% in all extranodal lymphomas (1). More than one-half of the cases of ocular adnexal lymphoma are mucosa-associated lymphoid tissue (MALT) lymphomas (2). MALT lymphoma, first described in 1983 by Isaacson and Wright (3), is believed to have a tendency to remain localized to the primary site for a long time (4). Therefore, local therapy has usually been applied for this disease (5, 6). Among several treatments, radiation therapy has been generally considered the most effective for localized disease (1, 4, 5, 7-9). The objective of our study was to analyze the characteristics of primary ocular adnexal MALT lymphoma (POAML), including its natural history, behavior of progression, prognostic factors, and treatment-related adverse effects.

Methods and Materials

Eighty-six patients with histologically proven stage I POAML treated with radiation therapy at National Cancer Center Hospital, Tokyo between 1990 and 2010 were retrospectively reviewed. The median age was 56 years (range, 18-85 years). There were 49 male (57%) and 37 female (43%) patients. The pathologic diagnosis of MALT lymphoma was established by biopsy or surgical resection sample. Staging workups included physical examination; complete blood count; magnetic resonance imaging (MRI) or computed tomography (CT) of both orbits; CT of the neck, thorax, abdomen and pelvis; and bone marrow biopsy. Tumors classified as stage I in this study were unilateral or simultaneous bilateral diseases that did not have extra-orbital extensions. Twelve patients had simultaneous bilateral lesions. These bilateral lesions were both treated by radiation therapy, and the total number of the eyes undergoing radiation as a primary therapy was 98. Additionally, all the 6 relapses in the contralateral eyes underwent radiation therapy. Therefore, the total number of eyes treated by radiation was 104 (unilateral primary, 74; bilateral primary, 12 × 2; contralateral relapses, 6). As for subsites of the 104 eyes, conjunctiva and eyelid involvement was seen in 46 eyes, lacrimal gland involvement in 7 eyes, and nonconjunctival/eyelid/lacrimal gland involvement in 51 eyes.

The total of 77 patients, including 66 with unilateral and 11 with bilateral lesions, were treated by radiation therapy alone (Table 1). Among the patients with unilateral tumors, 3 received chemotherapy followed by radiation therapy, and the other 5 underwent surgery (macroscopically complete excision) before radiation. Also, 1 bilateral tumor was treated with radiation and chemotherapy. Among those treated with radiation and chemotherapy, 2 patients had 4 or 6 cycles of cyclophosphamide, hydroxydaunorubicin, oncovin, and prednine (CHOP), 1 patient had 4 cycles of rituximab + CHOP (R-CHOP), and 1 patient had 1 cycle of cyclophosphamide, oncovin, and prednine. A total of 4 patients received chemotherapy.

The radiation doses varied between 30 and 46 Gy in 2 Gy per fraction, and the median dose was 30 Gy. No eyes were treated by a dose lower than 30 Gy. Direct appositional electron irradiation with 3 to 12 MeV was used in 41 eyes. The remaining 63 eyes were treated with 4- or 6-MV photon beams with a single anterior field or a wedged pair of anterior and oblique fields. A lens block made of lead was used in 39 of 104 eyes (photon beam, 27; electron beam, 12), and a bolus with 5 mm in water-equivalent thickness was used in 41 of 104 eyes (photon beam, 13; electron beam, 28).

Local relapse-free survival (LRFS) was calculated from the last day of radiation therapy until the date of the first documented relapse, with death and last follow-up visit without local relapse considered to be censored. Contralateral relapse-free survival (CRFS) was defined as the time from the last day of radiation therapy until the date of the first documented contralateral relapse, with death and last follow-up visit without contralateral relapse considered to be censored. In the analysis of contralateral relapses, 24 eyes of simultaneous bilateral diseases were not included because there was no contralateral eye for primary bilateral lesions. Overall survival (OS) was defined as the time from the last day of radiation therapy until the date of death of any cause or

Table 1 Patient characteristics

Characteristic	No.
Sex	
Male	49 patients (57%)
Female	37 patients (43%)
Age, y	
Median (range)	56 (18-85)
Bilateral presentation	12 patients
Contralateral relapse	6 patients
No. of irradiated eyes	104 eyes
Unilateral involvement	74 eyes
Bilateral involvement	24 eyes
Contralateral relapse	6 eyes
Primary site	
Conjunctiva and eyelid	46 eyes
Lacrimal gland	7 eyes
Nonconjunctiva/eyelid/lacrimal gland	51 eyes
Treatment	
RT only/chemo + RT/surgery + RT	94/5/5 eyes
Radiation dose, Gy	
Median (range)	30 (30-46)
Treatment (total no. of treated eyes: 104)	
X-ray	63 eyes
Electron beam	41 eyes
Shield	
Yes/no	39/65 eyes
Bolus	
Yes/no	41 (photon 13; electron 28)/63 eyes

Abbreviations: Chemo = chemotherapy; RT = radiation therapy.

until the date of the last follow-up visit for patients who were alive. Cataract incidence was calculated from the last day of radiation therapy to the date of cataract diagnosis. All the survival curves and the incidence of cataracts were calculated by the Kaplan-Meier method, with a statistical difference tested by log-rank test. A P value of less than .05 was considered to be statistically significant. All the statistical analyses were performed with Predictive Analytic Software (PASW), version 18.0 (SPSS Inc., Chicago, IL).

Results

The median follow-up time for all patients was 9 years (range, 0.9-22 years). The 5- and 10-year OS rates were 97.6% and 93.5%, respectively (Fig. 1). Also, the 5- and 10-year LRFS rates were 98.7% and 98.7%, and the CRFS rates were 97.0% and 90.8%, respectively. No patients died of the disease; the deaths of 6 patients were of causes unrelated to lymphoma. The number of total relapses was 10. Among them, 1 relapse occurred locally within the radiation field, and contralateral relapses were seen in 6 patients. The other 3 patients had distant relapse. The patient who experienced local relapse had had simultaneous bilateral tumors at presentation, and both tumors were treated by radiation therapy. Only her lymphoma in the conjunctiva of the right eye, with a size of several millimeters, relapsed 45 months after electron beam irradiation of 30 Gy. The 6 contralateral relapses were also treated by radiation therapy alone, and all those lesions were controlled with follow-up times of 3 to 12 years. Patients with tumor sizes ≥4 cm showed a greater risk of contralateral relapse, with 5- and 10-year CRFS of 100% and 55.6%, respectively, for tumors ≥4 cm, and 96.7% and 94.3%, respectively, for tumors <4 cm (P=.012) (Fig. 2). Other factors, such as sex, age, and tumor location, were not significant for relapse in the contralateral orbit.

The clinical characteristics of the simultaneous bilateral lesions are shown in Table 2. No clinical factors affected the bilateral lesions except for tumor size. Bilateral lesions were seen in 6.9% of the patients with tumors ≥1 cm and in 28.6% of the patients with tumors 1 cm (P=.007).

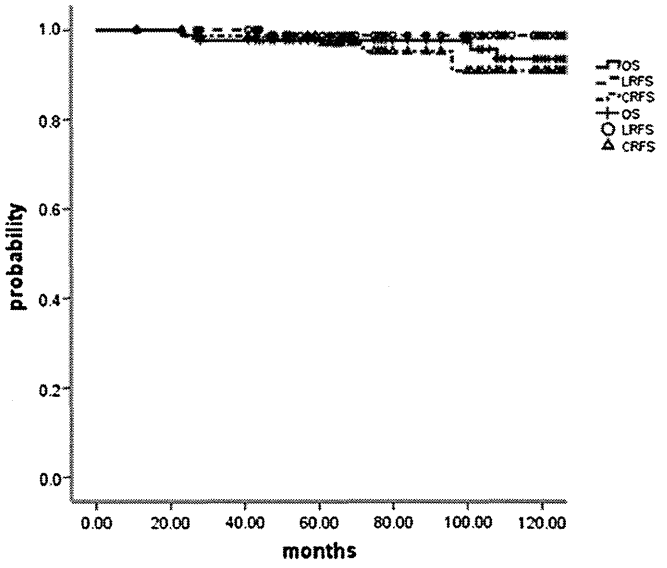

Fig. 1. Overall survival (OS) (n=86), local relapse-free survival (LRFS) (n=104), and contralateral relapse-free survival (CRFS) (n=74) in patients with primary ocular adnexal MALT lymphoma (5- and 10-year OS rates, 97.6% and 93.5%; LRFS rates, 98.7% and 98.7%; and CRFS rates. 97.0% and 90.8%, respectively).

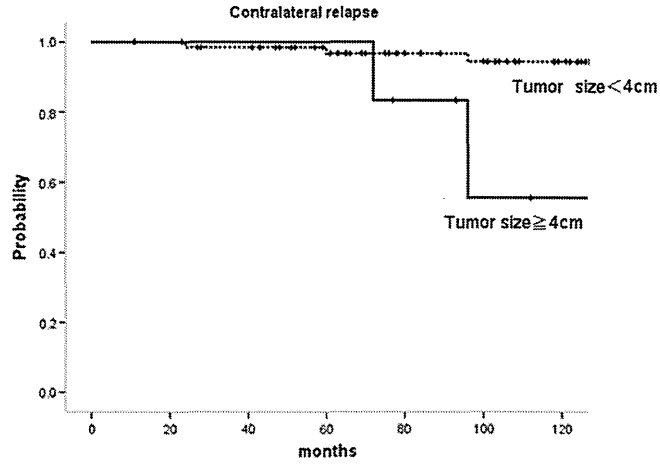

Fig. 2. Contralateral relapse-free survival rates according to tumor sizes.

Among the patients who experienced distant relapse, initial therapy was radiation alone for 2 patients and surgery followed by radiation for 1 patient. Of those, 2 experienced relapse at the mediastinum, and 1 at the left pleura. All of them underwent additional treatment. One patient with mediastinal disease was treated with 6 cycles of R-CHOP, and another patient with mediastinal disease underwent 6 cycles of R-CHOP followed by 30 Gy of radiation. The patient with pleural disease underwent surgery. All the patients achieved complete response with no evidence of disease at an additional 24 to 132 months of follow-up. There were no statistically significant prognostic factors that influenced distant relapse (Table 3).

Risk factors for cataract were retrospectively evaluated in 104 eyes, including eyes treated for primary diseases and 6 eyes treated for contralateral relapse. Cataracts occurred in 48 of 104 eyes. Of those, 31 eyes underwent surgery. Among 4 patients who were treated with chemotherapy including steroids, only 1 patient experienced a cataract without the use of a lens shielding. A lens-shielding technique was used in 39 of 104 eyes. Cataracts developed in 36 of the 65 eyes without lens shielding, with a 5-year cataract incidence of 50.9%, whereas 12 of the 39 patients with lens shielding experienced cataracts, with a 5-year cataract incidence of 27.4% (P=.037) (Fig. 3). The radiation dose was not a risk factor (65 eyes were treated with 30 Gy vs 39 eyes were

Table 2 Clinical features of unilateral and bilateral lesions

Feature	Unilateral	Bilateral	P value
Age, y	53.8	50.7	.51
Sex			.919
Male	42	7	
Female	32	5	
Size, cm			.007
<1	20	8	
≥1	54	4	
Location			.091
Conjunctiva	30	8	
Other than conjunctiva	44	4	

Table 3 Clinical features of distant metastasis

Feature	Distant relapse	Others	*P* value
Age, y	50.3	53.5	.725
Sex			.730
Male	2	47	
Female	1	36	
Size, cm			.629
<4	3	77	
≥4	0	6	
Location			.068
Lacrimal gland	1	5	
Other than lacrimal gland	2	78	

treated with >30 Gy; $P=.843$). Also, the use of a bolus did not influence the risk of cataracts.

Discussion

In this study, excellent LRFS of 98.7% in 5 and 10 years was achieved, and a moderate dose of 30 Gy was effective for stage I POAML (10-13). The predominant site of relapse was a contralateral orbit. However, even those contralateral relapses were controlled well by radiation therapy alone.

Most previous studies have analyzed the prognostic significance of tumor subsite at the conjunctiva or other locations (1, 9, 14). Some studies have suggested that tumor at the conjunctival location may have a better prognosis than those at other anatomic subsites of the orbit, whereas other studies have not found such a difference between the conjunctival location and other sites. In our study, we did not see any differences of prognosis between the conjunctiva and the other sites. Also, Nam et al (15) have stated that primary lacrimal involvement may be related to future relapse more frequently than other orbital subsites. In our study, there were 6 patients with lacrimal primary tumors. One patient had bilateral lacrimal involvement, and the total number of eyes with lacrimal involvement was 7 in 6 patients. Among them, only 1 patient with lacrimal tumor experienced distant relapse 12 years after radiation therapy. Also, a distant relapse rate according to conjunctiva and eyelid versus lacrimal gland and other orbital involvements was analyzed, and there was no significant difference between them. Because of the small number of the patients with distant relapse, a statistically significant influence of the primary orbital subsite on distant relapse could not be seen.

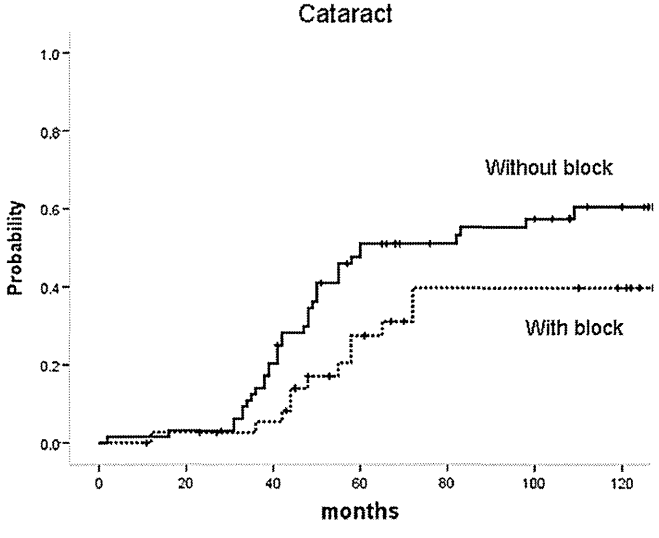

Fig. 3. Cumulative incidence of cataract according to whether lens shielding was used.

Some reports of POAML have shown distant relapse other than ocular relapse, and a possible role of immunochemotherapy in reducing distant relapse has been suggested. Hashimoto et al (13) reported that 30.6 Gy combined with rituximab successfully decreased the risk of systemic relapse. However, our study demonstrated, after extensive staging, that distant relapse of stage I POAML is rare, and immunochemotherapy seems to have only a small role in stage I POAML. Additionally, most reported series have demonstrated excellent OS, with only a small number of deaths attributed to POAML. The treatment with immunochemotherapy of all patients with localized POAML is cost demanding and is out of consideration. Contralateral orbital relapse was seen most often, but the median time to contralateral relapse was as long as 84 months after radiation therapy. Therefore, patients with stage I POAML must be followed up longer than 5 years, with meticulous attention to the contralateral eye. There are few reports on the management and prognosis of contralateral relapse of POAML. In our study, all the 6 contralateral relapses were treated by radiation therapy, and all were controlled for 3 to 12 years without local or extraorbital relapses. Goda et al (16) have stated that an isolated contralateral relapse of MALT lymphoma in the paired organ could be successfully managed with another course of RT and often did not result in further disease relapse in distant sites (16). Solitary contralateral relapse of stage I POAML should be treated by a repeated course of radiation therapy. Although anatomic site of tumor location, sex, and age were not significant for relapse in the contralateral orbit, the patients with tumor sizes ≥4 cm showed a greater risk for contralateral relapse more than 5 years after treatment. Therefore, long term follow-up is mandatory for patients with a larger tumor, attention being given to the contralateral eye.

In our series, primary bilateral lesions were small at presentation. POAML often presents as a salmon-pink lesion that is sometimes misdiagnosed as other ocular surface diseases, such as allergic or chronic conjunctivitis, and it is sometimes challenging to recognize the small tumor (17). There is a possibility that patients with bilateral lesions might draw the ophthalmologist's attention to the symptoms including irritation, epiphora, and mass sensation compared with patients with unilateral lesions. This might have resulted in an early diagnosis with relatively small size in our bilateral lesions. All of the bilateral lesions were controlled well by radiation except for 1 case of local relapse. Also, the NCCN Guidelines Version 1.2013 (18) recommends radiation therapy to both lesions in bilateral POAML.

A total dose of around 30 Gy in a conventional fractionation seems to be the present standard in radiotherapeutic management of POAML. Hashimoto et al (13) reported that 30.6 Gy combined with rituximab successfully decreased the risk of systemic relapse. By contrast, Tsang and coworkers (5) reported that for local control of POAML, the results of a slightly lower dose of 25 Gy in 30 patients with orbital lymphomas remained excellent. Recently, low-dose radiation has become increasingly used in the management of indolent non-Hodgkin lymphoma (NHL) (19-24). Fasola et al (25) recommended 2 Gy in 2 fractions as excellent treatment of NHL of the ocular adnexa for the purpose of disease control in patients with advanced stage disease, with the option of

reirradiation in the case of locoregional relapse. However, there are few data regarding how much the dose could be reduced safely in radical radiation therapy of POAML. Therefore, future clinical trials seem to be necessary to reduce the optimal doses in radiation therapy for POAML.

The use of the shielding block reduced the incidence of cataract, with a statistically significant difference. However, because cataract was effectively managed by surgery with a resultant restoration of vision, a shielding block must be inserted only in the lesions that can be treated with easy insertion of the shielding block. Although there was no evidence of any complication of cataract operations after radiation therapy during the follow-up period, cataract operations should be cautiously applied in clinics.

Conclusion

Local radiation therapy up to 30 Gy can attain excellent local control and overall survival of POAML. The predominant site of relapse was in the contralateral eye, which can be also controlled by local radiation. Because the median time to contralateral relapse was 84 months, long term follow-up of POAML is mandatory.

References

1. Martinet S, Ozsahin M, Belkacémi Y, et al. Outcome and prognostic factors in orbital lymphoma: a Rare Cancer Network study on 90 consecutive patients treated with radiotherapy. *Int J Radiat Oncol Biol Phys* 2003;55:892-898.
2. Naito Y, Tateya I, Hirano S, et al. Cortical correlates of vestibulo-ocular reflex modulation: A PET study. *Brain* 2003;126(Pt 7): 1562-1578.
3. Bonte I, Prigent F, Martinet C. [Orbital-palpebral edema]. *Ann Dermatol Venereol* 2003;130:655-656.
4. Tanimoto K, Kaneko A, Suzuki S, et al. Primary ocular adnexal MALT lymphoma: A long-term follow-up study of 114 patients. *Jpn J Clin Oncol* 2007;37:337-344.
5. Tsang RW, Gospodarowicz MK, Pintilie M, et al. Localized mucosa-associated lymphoid tissue lymphoma treated with radiation therapy has excellent clinical outcome. *J Clin Oncol* 2003;21:4157-4164.
6. Lee P. Clinical placement exchanges for pre-registration nursing students: Maximising opportunites. *Nurse Educ Pract* 2002;2:119-124.
7. Le QT, Eulau SM, George TI, et al. Primary radiotherapy for localized orbital MALT lymphoma. *Int J Radiat Oncol Biol Phys* 2002;52:657-663.
8. Bhatia S, Paulino AC, Buatti JM, et al. Curative radiotherapy for primary orbital lymphoma. *Int J Radiat Oncol Biol Phys* 2002;54: 818-823.
9. Uno T, Isobe K, Shikama N, et al. Radiotherapy for extranodal, marginal zone, B-cell lymphoma of mucosa-associated lymphoid tissue originating in the ocular adnexa: A multiinstitutional, retrospective review of 50 patients. *Cancer* 2003;98:865-871.
10. Smitt MC, Donaldson SS. Radiotherapy is successful treatment for orbital lymphoma. *Int J Radiat Oncol Biol Phys* 1993;26:59-66.
11. Lee SW, Suh CO, Kim GE, et al. Role of radiotherapy for primary orbital lymphoma. *Am J Clin Oncol* 2002;25:261-265.
12. Yahalom J. MALT lymphomas: A radiation oncology viewpoint. *Ann Hematol* 2001;80(Suppl 3):B100-B105.
13. Hashimoto N, Sasaki R, Nishimura H, et al. Long-term outcome and patterns of failure in primary ocular adnexal mucosa-associated lymphoid tissue lymphoma treated with radiotherapy. *Int J Radiat Oncol Biol Phys* 2012;82:1509-1514.
14. Coupland SE, Krause L, Delecluse HJ, et al. Lymphoproliferative lesions of the ocular adnexa: Analysis of 112 cases. *Ophthalmology* 1998;105:1430-1441.
15. Nam H, Ahn YC, Kim YD, et al. Prognostic significance of anatomic subsites: Results of radiation therapy for 66 patients with localized orbital marginal zone B cell lymphoma. *Radiother Oncol* 2009;90: 236-241.
16. Goda JS, Gospodarowicz MK, Pintilie M, et al. Long-term outcome in localized extranodal mucosa-associated lymphoid tissue lymphomas treated with radiotherapy. *Cancer* 2010;116:3815-3824.
17. Hata M, Miyamoto K, Ogino K, et al. Conjunctival extranodal marginal zone lymphoma of mucosa-associated lymphoid tissue in the fornix: Do not overlook conjunctival lymphomas. *Clin Ophthalmol* 2013;7:663-666.
18. NCCN Guidelines(R) Updates. *J Natl Compr Canc Netw* 2013;11: xxxii-xxxiii.
19. Ganem G, Cartron G, Girinsky T, et al. Localized low-dose radiotherapy for follicular lymphoma: History, clinical results, mechanisms of action, and future outlooks. *Int J Radiat Oncol Biol Phys* 2010;78: 975-982.
20. Ganem G, Lambin P, Socié G, et al. Potential role for low dose limited-field radiation therapy (2 x 2 grays) in advanced low-grade non-Hodgkin's lymphomas. *Hematol Oncol* 1994;12:1-8.
21. Sawyer EJ, Timothy AR. Low dose palliative radiotherapy in low grade non-Hodgkin's lymphoma. *Radiother Oncol* 1997;42:49-51.
22. Haas RL, Poortmans P, de Jong D, et al. High response rates and lasting remissions after low-dose involved field radiotherapy in indolent lymphomas. *J Clin Oncol* 2003;21:2474-2480.
23. Luthy SK, Ng AK, Silver B, et al. Response to low-dose involved-field radiotherapy in patients with non-Hodgkin's lymphoma. *Ann Oncol* 2008;19:2043-2047.
24. Haas RL, Poortmans P, de Jong D, et al. Effective palliation by low dose local radiotherapy for recurrent and/or chemotherapy refractory non-follicular lymphoma patients. *Eur J Cancer* 2005;41:1724-1730.
25. Fasola CE, Jones JC, Huang DD, et al. Low-dose radiation therapy (2 gy x 2) in the treatment of orbital lymphoma. *Int J Radiat Oncol Biol Phys* 2013;(5):930-935.

Journal of Radiation Research, 2014, 55, 780–787
doi: 10.1093/jrr/rru001 Advance Access Publication 23 February 2014

Dose error from deviation of dwell time and source position for high dose-rate ^{192}Ir in remote afterloading system

Hiroyuki OKAMOTO, Ako AIKAWA, Akihisa WAKITA, Kotaro YOSHIO, Naoya MURAKAMI, Satoshi NAKAMURA, Minoru HAMADA, Yoshihisa ABE and Jun ITAMI

Department of Radiation Oncology, National Cancer Center Hospital, 104-0045, Tokyo, Japan
Corresponding author. Tel: +81-3-3542-2511; Fax: +81-3-3545-3567; Email: hiokamot@ncc.go.jp

(Received 26 May 2013; revised 3 January 2014; accepted 6 January 2014)

The influence of deviations in dwell times and source positions for ^{192}Ir HDR-RALS was investigated. The potential dose errors for various kinds of brachytherapy procedures were evaluated. The deviations of dwell time ΔT of a ^{192}Ir HDR source for the various dwell times were measured with a well-type ionization chamber. The deviations of source position ΔP were measured with two methods. One is to measure actual source position using a check ruler device. The other is to analyze peak distances from radiographic film irradiated with 20 mm gap between the dwell positions. The composite dose errors were calculated using Gaussian distribution with ΔT and ΔP as 1σ of the measurements. Dose errors depend on dwell time and distance from the point of interest to the dwell position. To evaluate the dose error in clinical practice, dwell times and point of interest distances were obtained from actual treatment plans involving cylinder, tandem-ovoid, tandem-ovoid with interstitial needles, multiple interstitial needles, and surface-mold applicators. The ΔT and ΔP were 32 ms (maximum for various dwell times) and 0.12 mm (ruler), 0.11 mm (radiographic film). The multiple interstitial needles represent the highest dose error of 2%, while the others represent less than approximately 1%. Potential dose error due to dwell time and source position deviation can depend on kinds of brachytherapy techniques. In all cases, the multiple interstitial needles is most susceptible.

Keywords: dwell time; source position; ^{192}Ir; dose error; RALS

INTRODUCTION

The radioactive source and seed used in brachytherapy can emit photons or electrons in all directions. Dosimetrically, this means that the dose gradient around a brachytherapy source is very steep, and the dose decreases exponentially with the thickness of the material or tissue. Therefore, by implanting the source near or into the tumor region, high conformity of prescribed dose to the target and reduction of unwanted dose to healthy organs surrounding the tumor region can be obtained.

The use of CT or MR images in treatment planning for brachytherapy has been widely employed as image-guided brachytherapy (IGBT). Over the past few years, a number of studies have been conducted on various IGBT techniques [1–4]. Dose distributions can be customized to fit the target for each patient by referring to actual anatomy from CT or MR images instead of film-based planning. Furthermore, recently, sophisticated dwell time optimization techniques, such as graphical optimization and inverse planning anatomy-based dose optimization, has been implemented in commercial treatment planning systems (TPSs) [5–9].

Treatment parameters (including dwell times and dwell positions of the radioactive source calculated by TPSs) are transferred to the treatment machine, such as a remote afterloading system (RALS), manufactured e.g. by Nucletron, an Elekta company (MicroSelectron®, Stockholm, Sweden), Varian Medical Systems Inc. (VariSource™, Palo Alto, CA, USA), or Eckert & Ziegler Bebig SA (MultiSource®, Seneffe, Belgium). The RALS should provide high precision control of the movement of the radioactive source as planned in terms of the dwell times and dwell positions in the applicators in which the source moves. Mechanical accuracies of movement of the radioactive source have been referred to in some quality assurance/quality control (QA/QC) guidelines for high-dose-rate (HDR) RALS [10–13]. For example, AAPM Task Group 40 and Task Group 56 refer to a tolerance of source positioning of ±1 mm [10, 11]. ESTRO Booklet No. 8 recommend an action level of source positioning accuracy

of ±2 mm [12]. The tolerance or action level can be applicable for the scheduled QA/QC treatment machine. However, it is not obvious how these figures relate to clinical practice, and they lack practical value in terms of clinical influence. It has been further suggested that these values can be applied to all of the irradiation techniques in brachytherapy, such as surface-mold and interstitial brachytherapy, etc. Actually, dose error due to deviation of the source position depends on the distance from the source according to the inverse square law. A large dose error can be observed near the source, but the dose error far from the source is less.

Similarly, the impact of dose change caused by dwell time error can be expected to be linearly dependent on total dwell time. For instance, a tiny dwell time error can have a large impact in the case of low dwell time. In particular, the graphical optimization and inverse-planning anatomy-based dose optimization of the commercially available TPSs performs calculations of the dwell times without putting a lower limit on dwell time. Therefore, it is important to investigate dose error for such brachytherapy techniques, which freely use a low dwell time.

Dose error from mechanical uncertainties of movement of the source can depend on the kind of irradiation technique used, and its clinical influence is not fully understood. Our purpose in this study was to evaluate the dose error for clinical treatment plans involving a range of irradiation applicators/catheters, such as cylinder, tandem/ovoid, tandem/ovoid with a small number of interstitial needle applicators ('Combination-brachytherapy'), multiple interstitial needle applicators, and surface-mold applicators for scalp tumors.

In this study, deviations in dwell time and source position were measured for a number of techniques. Finally, the influence of the dose error due to both deviations was investigated for actual treatment plans involving the various applicators or catheters listed above.

MATERIALS AND METHODS

Measurements of deviation of dwell time and source position

For ^{192}Ir HDR-RALS (MicroSelectron® V2, Nucletron, an Elekta company), the deviation in dwell time ΔT and source position ΔP were measured for a range of techniques [12–16]. For two measurements, the air kerma strength was ~30.0 mGy m^2 h^{-1}. The Nucletron RALS has a nominal time resolution of 0.1 s. As shown in Eq. (1), dwell time, T_m was obtained from the amount of electric charge measured by a well-type ionization chamber (WIC) and an electrometer (HDR-1000 plus and MAX-4000, Standard Imaging Inc., Middleton, WI, USA). The correction factor k_{TP} was applied to convert the cavity air mass at the reference conditions (temperature T_0 22°C and pressure P_0 101.3 kPa) [13].

Dwell time T_m can be obtained from the amount of net electric charge ($M - M_{EF}$) and the current A_0 of the WIC during the irradiation, as shown in the following equation.

$$T_m = \frac{M - M_{EF}}{A_0} \quad (1)$$

M_{EF} means amount of electric charge in the end effect of a source, and it can be regarded as a constant independent of dwell time. Therefore, a standard deviation of dwell time T_m can be equal to that of M/A_0. The dwell time deviation ΔT was defined as a maximum value for a standard deviation of 10 measurements of M/A_0 for nominal dwell time T of 0.1, 0.2, 0.5, 1.0, 5.0, 15.0 and 30.0 s.

The deviations in the source positions were measured with two methods. One method involved measuring the position of the source with a source position check ruler device specifically developed for MicroSelectron® and provided by Nucletron, an Elekta company. The MicroSelectron® was set up to place the source in a certain position via the ruler connected by a straight transfer tube. By reading the actual source position, the standard deviation of the position deviation was obtained. A total of 11 measurements were performed to obtain a standard deviation. The other method involved irradiation of radiographic film (EDR2, Carestream Health Inc., Rochester, NY, USA) with applicators tightly attached to it. Irradiation was performed with 2-cm gaps between the dwell positions, and the number of gaps was 198. The exposed films were digitized with an EPSON ES-8500 flatbed scanner under resolution conditions of 600 dpi (equivalent to 0.042 mm/pixel) and a 16-bit gray scale. The digitized images were analyzed using film QA software (DD-system Ver. 10.21, R-TECH Company, Tokyo, Japan) as shown in Fig. 1. The source position deviation ΔP was defined as the maximum of a standard deviation for two tests (ruler and radiographic film).

Evaluation of dose error in single catheter method

As shown in Fig. 2, we calculated the dose errors at the points of interest due to deviations in both dwell time ΔT and source position ΔP, using the methods as described in the previous section. Two deviations were used as a standard deviation (according to Gaussian distribution) in the development environment of Microsoft Visual Studio 2010 instead of the commercial TPS. Dose calculation with a grid size of 1.0 mm was performed according to AAPM TG-43 protocol [17–19], as is typically used for dose calculation in brachytherapy TPS. Points of interest were placed at a distance L from each dwell position in the perpendicular direction of a catheter. A total of 10 dwell positions with a 2.5-mm distance from each source was investigated. Dose deviations were defined as the mean value for a standard deviation of the dose at the points of interest in 10 trials.

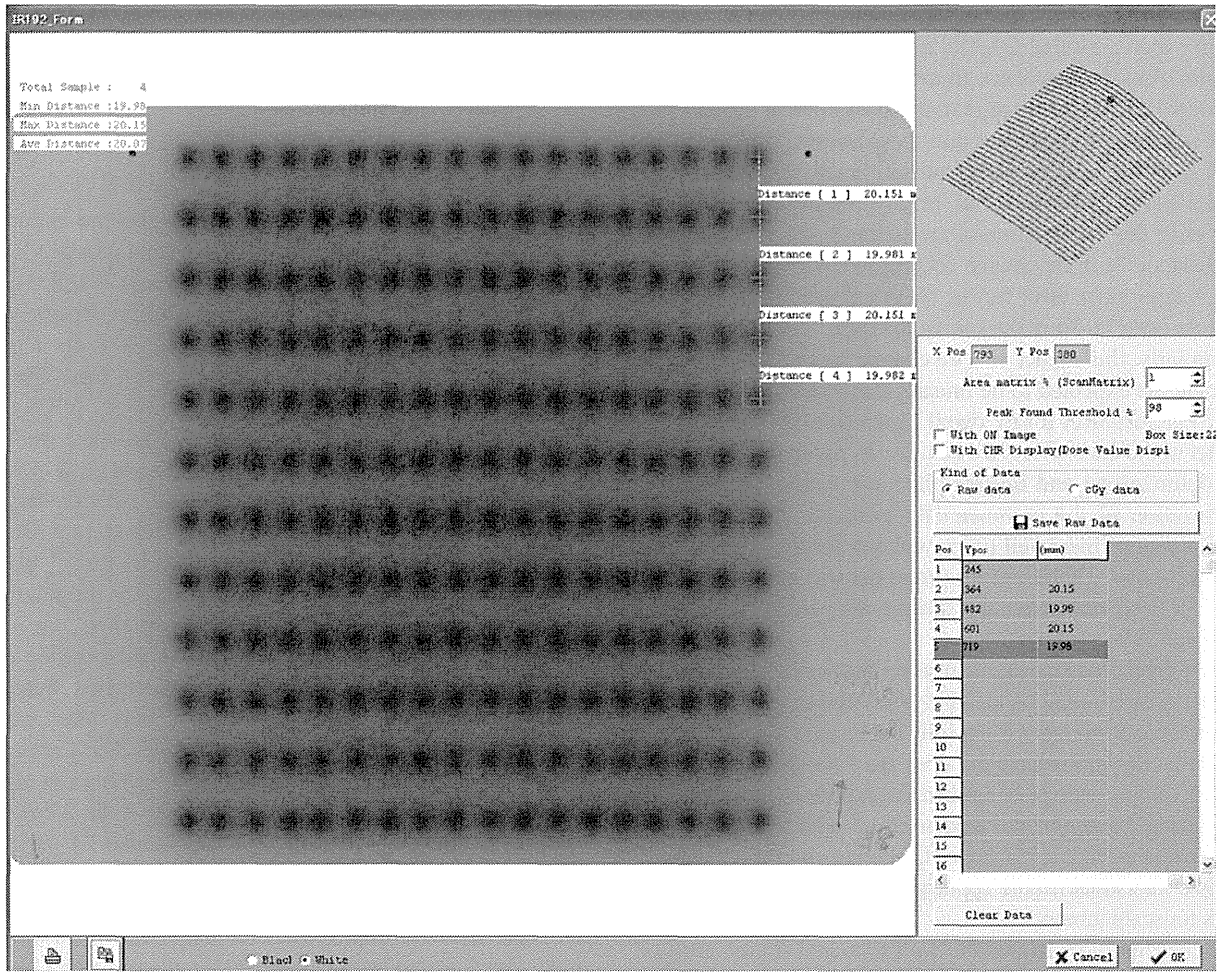

Fig. 1. Radiographic film EDR2 (Carestream Health Inc.) was analyzed for the measurement of source position accuracy using film QA software DD-system Ver. 10.21 (R-TECH Company).

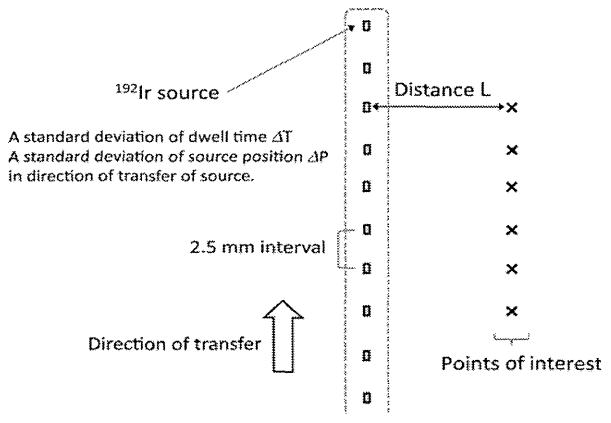

Fig. 2. Dose errors at points of interest for a single catheter calculated according to the AAPM TG-43 protocol [17–19] due to the two deviations: dwell time deviation ΔT and source position deviation ΔP.

Evaluation of dose calculation error in various clinical treatment plans

Dose error at the points of interest is affected by two factors: dwell time and distance of the point of interest from the source. In order to evaluate the influence of the two deviations, ΔT and ΔP, for a clinical treatment plan, we measured the dwell times and distance to points of interest in the actual treatment plan for a range of applicator types, such as cylinder, tandem/ovoid, combination-brachytherapy, multiple interstitial needle applicators, and surface-mold applicators for scalp tumors, in TPS Oncentra Brachy Ver. 4.1.0.132 (Nucletron, Veenendaal, Netherland). Table 1 provides information about the treatment plans for the various applicator types investigated here.

As time passes, dwell times for the same treatment plan must be increased in order to compensate for the decay of the radioactivity source (half-life of ^{192}Ir = 73.83 d). In other words, air kerma strength is higher, e.g., just after the replacement of an ^{192}Ir source. A maximum value S_K of 48.56 mGy m^2 h^{-1} was

Table 1. Treatment plans using various kinds of applicators or catheters

Applicators or catheters	# treatment plans	Prescribed dose (Gy)	Method of optimizing dose distribution
Cylinder	16	6	Dose point optimization to 5 mm under vaginal surface
Tandem/ovoid	17	6	Manchester system
Combination-brachytherapy	9	6	Inverse planning based on dose–volume histogram and graphical optimization
Multiple interstitial needle applicators	8	6	
Surface-mold for scalp tumor	5	2–2.5	Dose point and graphical optimization

obtained from the 43 measurements taken between February 2002 and December 2012 in our institute (average ± 1SD, 42.21 ± 3.06 mGy m^2 h^{-1}). Dwell times for all of the treatment plans listed in Table 1 were recalculated using the maximum S_K of 48.56 mGy m^2 h^{-1}, because a large dose error can be observed in the case of low dwell time.

In this study, the distance to the point of interest was defined by the equation below. We used the geometrical averaged distance r_g of the point of interest from catheter, r_g.

$$r_g = \sqrt{V_{100\%} / \sum_i \pi l_i} \quad (2)$$

This equation can be derived from $\sum \pi r_g^2 \times l_i = V_{100\%}$. $V_{100\%}$ means the irradiated volume receiving the prescribed dose or more, and it can be obtained from the dose–volume histogram in the TPS. The l_i is assumed to be the length of treatment region of the ith catheter. The gap between the dwell positions was set to a 2.5-mm interval. Therefore, the length of treatment region l_i could be expressed as a multiplication of the 2.5 mm interval by the number of dwell positions.

RESULTS

Measurements of deviation of dwell time and source position

Dwell time deviation was measured with a WIC. The standard deviations of dwell time for 10 measurements are shown in Table 2. From these results, the maximum standard deviation was found to be 32 ms for a dwell time of 30.0 s.

Deviation of the source position in the Nucletron RALS was measured using the two methods. The standard deviation of the source position was 0.12 mm and 0.11 mm in measurements using either the source position check ruler device ($n = 11$) or radiographic film ($n = 198$), respectively. The dwell time and source position deviation in this study were regarded as a standard deviation according to Gaussian distribution, $\Delta T = 32$ ms and $\Delta P = 0.12$ mm (worst case scenario).

Table 2. Dwell time deviation for Nucletron RALS measured with a WIC

Dwell time (s)	0.1	0.2	0.5	1.0	5.0	15.0	30.0
Deviation (ms)	18	17	23	23	29	23	32

Dose error in a single catheter by calculation

Figure 3a depicts the calculated dose errors as a function of dwell time with points of interest placed at a fixed distance of 5 mm with the measured two deviations, using $\Delta T = 32$ ms and $\Delta P = 0.12$ mm as the standard deviation according to the Gaussian distribution. Dose errors were calculated with three conditions: with either ΔT, ΔP, or both of them to reveal the contribution of each deviation to the total dose error. Using only ΔP, the dose error was constant independent of the dwell time. Using only ΔT, the dose error decreased with an increased dwell time. For both two deviations, the dose error also decreased with an increase in dwell time, and was a composite of the graphs when using only ΔP and only ΔT. Figure 3b depicts the calculated dose errors as a function of distance L to the point of interest with a fixed dwell time of 2 s and the two measured deviations, $\Delta T = 32$ ms and $\Delta P = 0.12$ mm generating the standard deviation according to Gaussian distribution. Dose errors were also calculated according to these assumptions in Fig. 3a. With only ΔP, the dose error decreased with an increase in distance L to the point of interest. The dose error approached zero, because ΔP is less influential for a point distant from the source. Using only ΔT, the dose error remained constant, because dose was linearly proportional to the dwell time. With both deviations, the dose error also decreased with increase in distance to the point of interest, and was a composite of the graphs with only ΔP and only ΔT.

As shown in Fig. 3, the dose error depended on two factors: dwell time and distance to the point of interest. Figure 4 depicts a 2D-plot of the dose errors with the two measured deviations, $\Delta T = 32$ ms and $\Delta P = 0.12$ mm. As shown in the figure, a high dose error could be observed near the source for a small dwell time.

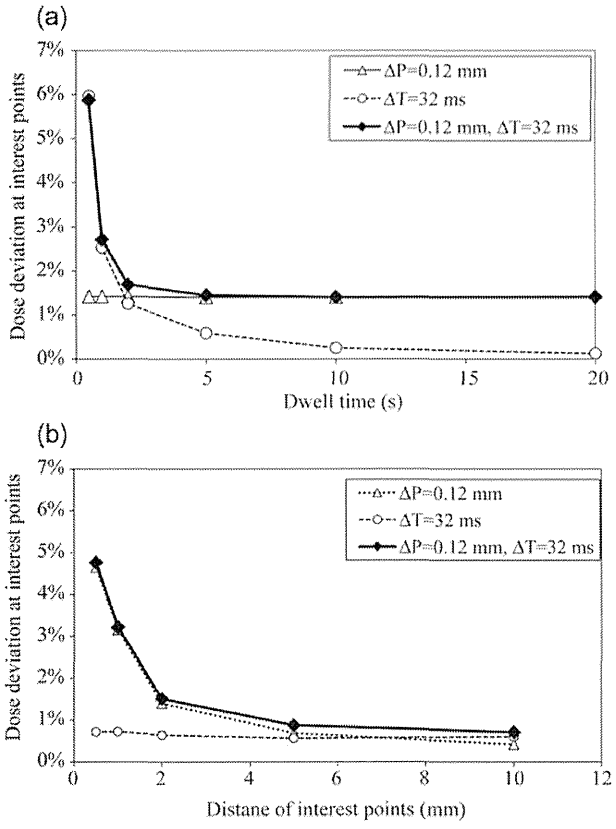

Fig. 3. Dose error for $\Delta T = 32$ ms and $\Delta P = 0.12$ mm: (**a**) dose error at points of interest placed at a fixed distance of 5 mm as a function of dwell time by calculation. (**b**) Dose error for a fixed dwell time of 2 s as a function of distance to points of interest by calculation.

Dwell time and distance to the point of interest for clinical treatment plans

Figure 5 depicts the box-and-whisker plot of dwell times per dwell position in the actual clinical treatment plans as described in Table 1. The median dwell time for each dwell position was 27.18, 19.10, 5.74, 0.73 and 0.95 s for the cylinder, tandem/ovoid, combination-brachytherapy, multiple interstitial needle applicators, and surface-mold applicators for scalp tumors, respectively. The lower quartile of dwell times was 20.96, 13.26, 1.97, 0.34 and 0.69 s, respectively. For instance, Fig. 6 depicts a distribution of dwell times for the multiple interstitial needle applicators ($n = 8$ treatment plans).

Figure 7 depicts the box-and-whisker plot of the geometrical averaged distance to the point of interest r_g derived from Eq. (2) for the clinical treatment plans (see Table 1). The median value of r_g was 30.73, 29.06, 17.01, 8.08 and 20.10 mm in the cylinder, tandem/ovoid, combination-brachytherapy, multiple interstitial needle applicators, and surface-mold applicators for scalp tumors, respectively. The lower quartile of r_g was 30.14, 28.51, 16.37, 7.44 and 15.70 mm, respectively. Furthermore,

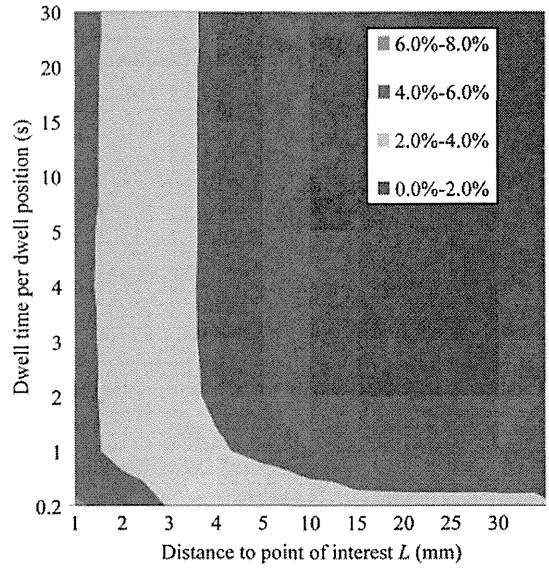

Fig. 4. 2D-plot of dose error for dwell times and distance to point of interest L for $\Delta T = 32$ ms and $\Delta P = 0.12$ mm.

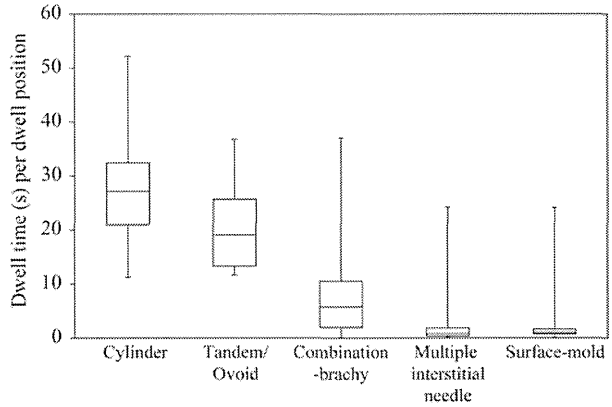

Fig. 5. The box-and-whisker plot of the dwell times per source position for the clinical treatment plans (see Table 1).

minimum r_g was 27.03, 27.22, 14.72, 6.47, and 15.29 mm, respectively.

Potential dose error for clinical treatment plans

We adopted the results of the dose error for a single catheter by calculations from clinical treatment plans. We introduced the median value of Figs 5 and 7 as a representative expression of the treatment plans. This condition assumed that the dwell time and the distance to the point of interest for all activations can be considered equivalent to the median value. Table 3 lists the potential dose errors that were obtained from the 2D-plot of the dose error indicated by the two median values.